



Synthesis, characterization of silicate intercalated and evaluation of their antimicrobial activity

Sahli Fatima Zohra^{1*}, Sassi Mohamed², Labbaci Abdallah¹, Hocine Laredj³

¹Water and Environment Laboratory, Department of Processes Engineering, University of Hassiba Benbouali Chlef

²Material Chemistry Laboratory - Department of Chemistry, University of Oran Ahmed Ben Bella, 3100 Oran, Algeria

³Laboratory of Agro-Biotechnology and Nutrition in Semi-Arid Areas, Faculty of Sciences of Nature and Life, University of Ibn Khaldoun, Tiaret

Key words: Synthesis, Lamellar polysilicate, Intercalation, Anti-bacterial agent, Pollution.

<http://dx.doi.org/10.12692/ijb/16.2.373-381>

Article published on February 24, 2020

Abstract

This study focuses on the development of antimicrobial polysilicate to clean water from pathogenic bacteria. A new silicate intercalated synthetic antibacterial is described. The layered sodium silicate kanemite was synthesized under hydrothermal conditions. The kanemite obtained is intercalated by organic molecules (alkyltrimethylammonium). The products obtained are characterized by X-ray diffraction (XRD), infrared spectroscopy (FTIR) and scanning electron microscopy (SEM). The antibacterial activity of the materials obtained is evaluated by measuring the minimum inhibitory concentration (MIC) by exposing them to the two bacteria strains, i.e. *Escherichia coli* and *Staphylococcus aureus*, at different concentrations. The C16TMA-kanemite demonstrates very high antimicrobial activity against the two microorganisms tested as well as the material use in water treatment. Indeed, it exhibits a minimum inhibitory concentration of 0.05g per 5ml of physiological water during 15 minutes.

*Corresponding Author: Sahli Fatima Zohra ✉ fatima191080@yahoo.fr

Introduction

Bacteria are unicellular microorganisms without nuclei, they are classified as prokaryotes because they do not have a nuclear membrane, their diameter is less than $1\mu\text{m}$. In recent years, the synthesis of materials with antibacterial activity has brought great interest to researchers because of the global concern for public health (Ma YL *et al.*, 2004). Clays are generally the most used materials in the preparation of antibacterial composite materials (Yamada *et al.*, 1991). Indeed, the compensation cations present in the interfoliar space can be exchanged by ions which can generate an antibacterial activity. This results in a family of antibacterial composite materials (Herrera *et al.*, 2000). Kanemite (Johan *et al.*, 1972) ($\text{NaHSi}_2\text{O}_5 \cdot 3\text{H}_2\text{O}$) is a layered polysilicate, the layers of which are composed of monolayer sheets of SiO_4 tetrahedra. It is capable of exchanging the sodium ions intercalated between the layers. With a consequent increase of the interlayer distance.

Magadiite, included interlayer exchangeable cations which were often hydrated. Magadiite structure was composed of multiple negatively charged sheets of SiO_4 tetrahedra with abundant silanol-terminated surfaces. This type of reaction concerns the exchange of interlamellar cations of polysilicates in layers with other cations such as protons (Rojo *et al.*, 1988; Heinrich Thiesen *et al.*, 2002; Wang *et al.*, 2017).

Magadiite has an interesting cation exchange capacity (CEC) that has been applied to ion exchange. The exchange of sodium ions with protons to form silicic acid. On the other hand, different types of cations or large quaternary ammonium ions, it has therefore proved to be a good candidate for the manufacture of organic-inorganic composites (Ogawa *et al.*, 1998; Ogawa *et al.*, 1999; Okutomo *et al.*, 1999; Ruiz-Hitzky *et al.*, 2011; Ren *et al.*, 2015; Wang *et al.*, 2017).

The lamellar polysilicates have outstanding cation exchange and intercalation properties which undoubtedly enable them to develop a new family of novel antibacterial materials.

This paper deals with the synthesis, and the characterization of kanemite intercalated by alkyl trimethylammonium, this material obtained (C_{16}TMA kanemite) is subjected to different characterizations: X-ray diffraction (XRD), infrared spectroscopy (FTIR), scanning electron microscopy (SEM) and the evaluation of antibacterial activity.

Materials and methods

Materials

The main reagents used during this work were Colloidal silica ludox AS 40 (40% SiO_2 , 60% H_2O) from Dupont, ethanol (96wt%) from Doks Alcohols, sodium hydroxide (NaOH) from Fluka and cetyltrimethylammonium chloride (25% solution in water) from Aldrich.

Analytical methods

X-ray diffraction was carried out with $\text{CuK}\alpha$ monochromatic radiation using a diffractometer Philips PW1830. The scanning microscopy analyses were performed on a model LEO. Sterioscan 440 electron microscope in the backscattered mode. The infrared spectra were recorded using KBr disc method on a spectrometer Perkin Elmer FT-IR in the region $400\text{--}4000\text{cm}^{-1}$. The UV-VISIBLE analysis was carried out on a SHIMADZU UV-VIS 1202 spectrophotometer.

Synthesis of kanemite

The kanemite was prepared by the method described by Beneke and Lagaly (Beneke *et al.*, 1977). A mixture of amorphous silica and NaOH (SiO_2 : NaOH = 1:1) was dissolved under stirring in 100 mL of methanol with cooling. It was then dried at 100°C for 2 week. After this, the dried material was calcined at 700°C for 5.5h. After cooling to room temperature the product obtained was dispersed in the water, filtered, and air dried. It is then characterized by X-ray powder diffraction, FTIR spectroscopy and Scanning Electron Microscopy (SEM).

Preparation of C_{16}TMA -kanemite material

C_{16}TMA -Kanemite material was prepared by an ion – exchange method of interlayer Na^+ cations with

C₁₆TMA cations (Kimura *et al.*, 2000). Kanemite (1.0 g) was added to 0.1M aqueous C₁₆TMACl solution (200 ml). The mixture obtained was stirred for 2 days at room temperature.

The resulting solid products were separated by centrifugation and dried in air. The ion exchange reaction is described by the following equation:



Measurement of the minimal inhibitory concentration

To determine the minimum inhibitory concentration of C₁₆TMA-kanemite one follows the following steps: Different masses of C₁₆TMA-kanemite taken separately with 5 ml of nutrient agar contained in a sterile tube are incorporated.

The mixture is poured into a sterile petri dish, and strains of *Staphylococcus aureus* and *Escherichia coli*, which are also taken separately on the agar, are seeded with a non-incorporated nutrient agar seeded with the same strains as a witness. The petri dishes are incubated at 37 °C for 24 hours (Boukara *et al.*, 2008).

Study of antibacterial activity in water

The measurement of microbial kill requires the ability to measure the number of surviving microorganisms over time after exposure to the antibacterial agent.

We will study the behavior of these bacteria (*Staphylococcus aureus* and *Escherichia coli*) in physiological water vis-à-vis C₁₆TMA-kanemite. We will proceed as follows:

A bacterial suspension of *Staphylococcus aureus* and *Escherichia coli* is Prepared in a tube containing 5ml of physiological saline having a fixed optical density of 0.78 for the two strains. 0.1ml of this tube is taken and sowed in a tube with 10ml of nutrient broth. In the same first tube, the mass found when determining the MIC of C₁₆TMA-kanemite is used.

The mixture is shaken for 30 minutes while 0.1 ml of the tube is withdrawn every 5 minutes using a sterile

syringe and is seeded in a tube containing 10 ml of nutrient broth.

The seed tubes are incubated at 37 °C for 24 hours, then the optical density of growth was measured by spectrophotometer (UV-VIS-1202 SHIMADZU) at 600 nm (Jean, 1993).

Anti-bacterial activity of C₁₆TMA-kanemite against *Staphylococcus aureus* and *Escherichia coli*

After 24 hours of incubation, the optical density (DO) of the two strains is read using a UV-Vis spectrophotometer at 600 nm.

We will express the antibacterial activity of C₁₆TMA-Kanemite synthesized according to the number of bacteria (number expressed in Colony-Forming Unit per millimeter CFUml⁻¹). The transformation of DO into UFC / ml is made by the relation:

$$\text{DO} = 0.7 \rightleftharpoons 10^8 \text{ UFC/ml} \quad (\text{Hamadi } et al., 2009).$$

The antibacterial activity C₁₆TMA-kanemite turns out to be very different with respect to the two bacterial strains.

Results and discussion

X-ray diffraction

The X-ray diffraction pattern of kanemite is represented in Fig.1.

It confirms the identity of the product obtained as kanemite in very good agreement with the results of the literature (Beneke *et al.*, 1977).

The diffraction peaks exhibit high intensities, indicating a good crystallinity of the material obtained and no impurity is detected.

The peak at $2\theta = 8.65^\circ$ is attributed to the reflection (020) and corresponds to a base spacing of 1.02 nm, The Fig. 2 shows the x-ray diffraction spectrum of C₁₆TMA-kanemite. It is clear that the intercalation of kanemite with C₁₆TMA ions significantly affects its structural integrity. Indeed, the ion exchange reaction

of kanemite with C_{16} TMA cations leads to the complete disappearance of the (001) line corresponding to the basal spacing, d_{001} , as well as its harmonic (002) line Fig. 2. This important result

indicates that the kanemite material is completely exfoliated after intercalation of C_{16} TMA cations. This confirms that the exchange reaction has taken place.

Table 1. Minimum Inhibitory Concentration of C_{16} TMA-kanemite Versus *Staphylococcus aureus* and *Escherichia coli*.

Mass of C_{16} TMA-kanemite g	<i>Staphylococcus aureus</i> inhibition	<i>Escherichia coli</i> inhibition
$3 \cdot 10^{-2}$	No inhibition	No inhibition
$4 \cdot 10^{-2}$	No inhibition	inhibition
$5 \cdot 10^{-2}$	inhibition	inhibition
$6 \cdot 10^{-2}$	inhibition	inhibition

Table 2. Antibacterial activity of C_{16} TMA-kanemite Against *Staphylococcus aureus* (Tears: DO = 0.60 = $8.57 \cdot 10^7$ CFU/ml).

Time (min)	DO (600nm)	N_0 (CFU/ml)
0	0.005	$0.71 \cdot 10^6$
5	0.020	$2.85 \cdot 10^6$
10	0.078	$11.14 \cdot 10^6$
15	0	0
20	0	0
25	0	0
30	0	0

Infrared absorption spectrum

The infrared spectrum of kanemite is represented in Fig. 3. It shows a signal at 3570 cm^{-1} associated with the vibrations of the free silanol $\equiv\text{Si-OH}$ of the silicate layer and a broad vibration band at 3445 cm^{-1}

attributed to OH groups forming hydrogen bonds or to OH groups of interlamellar water. Another signal is observed at about 1630 cm^{-1} which indicates the presence of physisorbed water (frequency of shearing of the water molecules).

Table 3. Antibacterial activity of C_{16} TMA-kanemite against *Escherichia coli*. (Tears: DO 0.530 = $7,571 \cdot 10^7$ CFU/ml).

Time (min)	DO (600nm)	N_0 (CFU/ml)
0	0.503	$7.18 \cdot 10^7$
5	0.213	$3.04 \cdot 10^7$
10	0.205	$2.92 \cdot 10^7$
15	0.215	$3.01 \cdot 10^7$
20	0.190	$2.71 \cdot 10^7$
25	0.183	$2.61 \cdot 10^7$
30	0.195	$2.78 \cdot 10^7$

The absorption bands corresponding to the vibrations of the Si-O bond are observed at 1170, 1046 and 456 cm^{-1} . A series of weak bands between 900 and 500

cm^{-1} are to be noted; these bands are detectable in the spectrum of synthetic hydrated silica $\text{H}_2\text{Si}_2\text{O}_5 \cdot (2\text{SiO}_2 \cdot \text{H}_2\text{O})$, but are absent from the spectrum of

amorphous silica. Fig. 4 shows the infrared spectrum of the C₁₆TMA-kanemite. In addition to the vibration bands of kanemite, it shows the absorption bands due to the asymmetric stretching vibration of methylene groups (CH₂) at 2917cm⁻¹ and the symmetrical one at about 2850 cm⁻¹. The bands appearing between 900

and 950 cm⁻¹ arise from CN⁺ stretching vibrations and CH deformation.

The band at 1471 cm⁻¹ is associated with shearing of CH₂ groups, while that at 1320 cm⁻¹ is characteristic of CH shearing of a conformation.

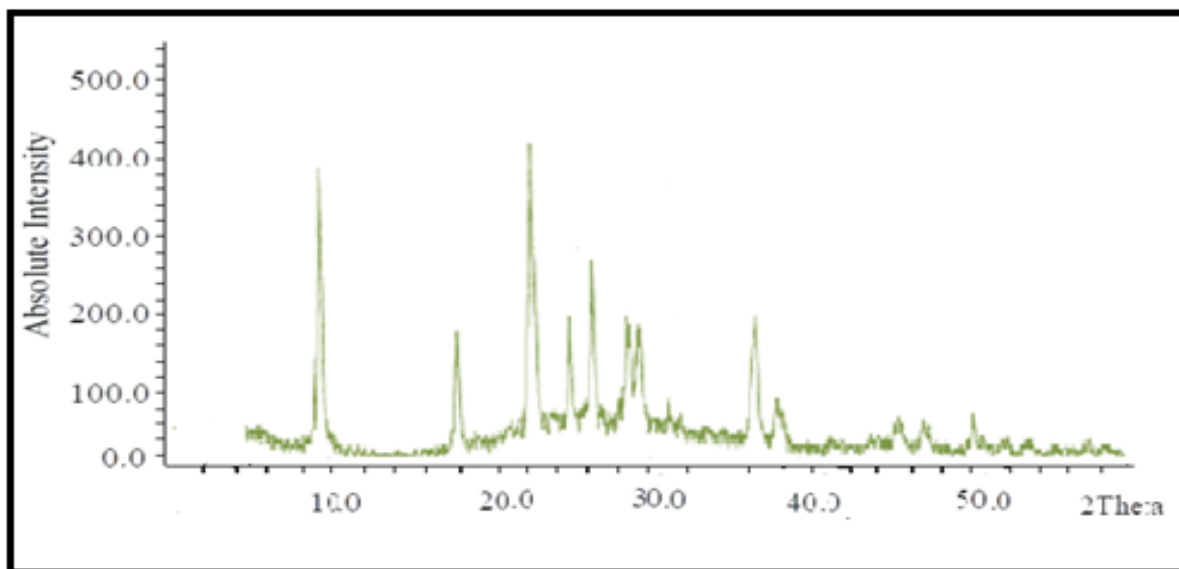


Fig. 1. X-ray diffractogram of kanemite.

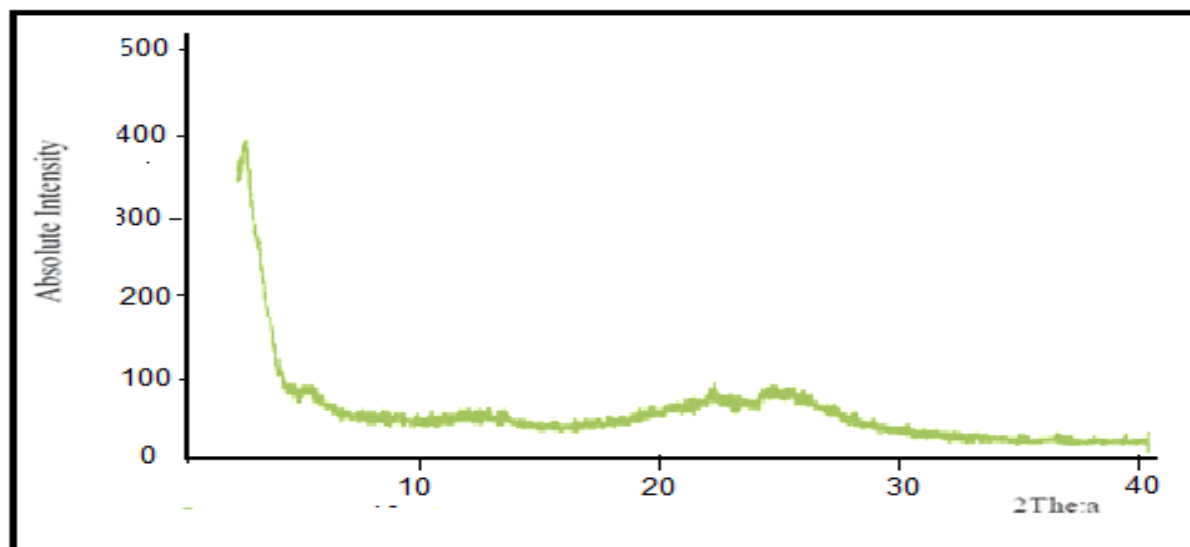


Fig. 2. X-ray diffractogram of C₁₆TMA-kanemite.

Scanning electron microscopy (SEM)

The morphology of kanemite and C₁₆TMA-kanemite such as synthesized is represented in Fig. 5. It is well observed that these powders are composed of agglomerates, which are themselves composed of aggregates of heterogeneous sizes. The kanemite crystallites are of large size ranging from 2-5µm.

Measurement of the minimum inhibitory concentration of C₁₆TMA-kanemite versus *Staphylococcus aureus* and *Escherichia coli*

After incubation of 24 of the two strains, the results are described in the following tables: Knowing that we have seen growth in the petri dishes as a support Table 1 Comparing the results obtained during the

determination of the MIC Table1, it is noted that C_{16} TMA-kanemite shows an inhibitory effect slightly elevated against *Escherichia coli* against

Staphylococcus aureus as this bacterium is known for its resistance to the products amines (Gaudy *et al.*, 2005).

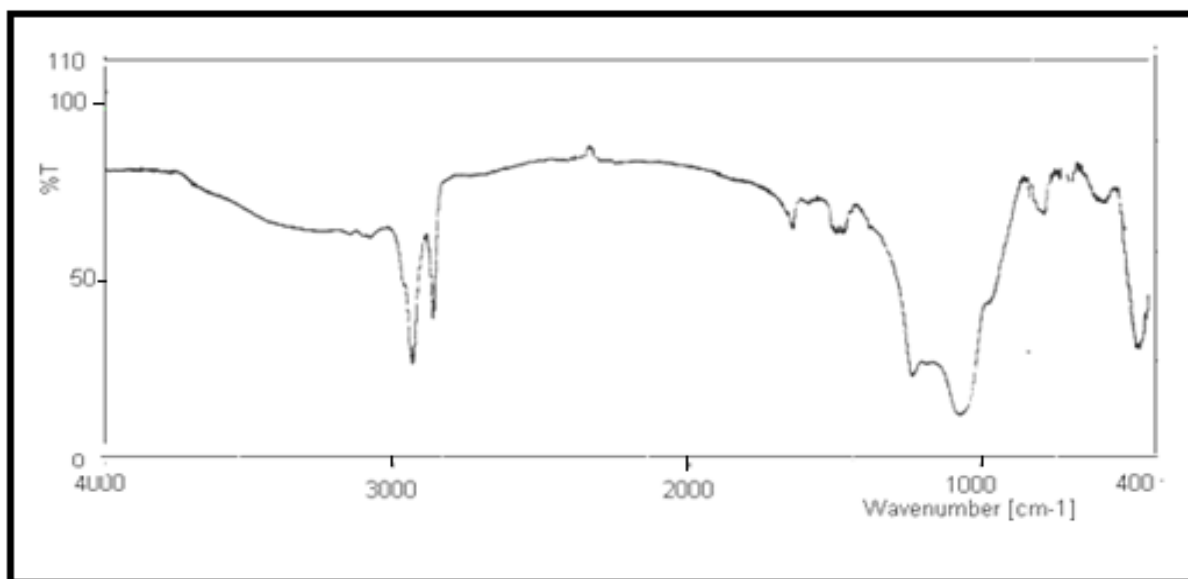


Fig. 3. IR spectrum of kanemite.

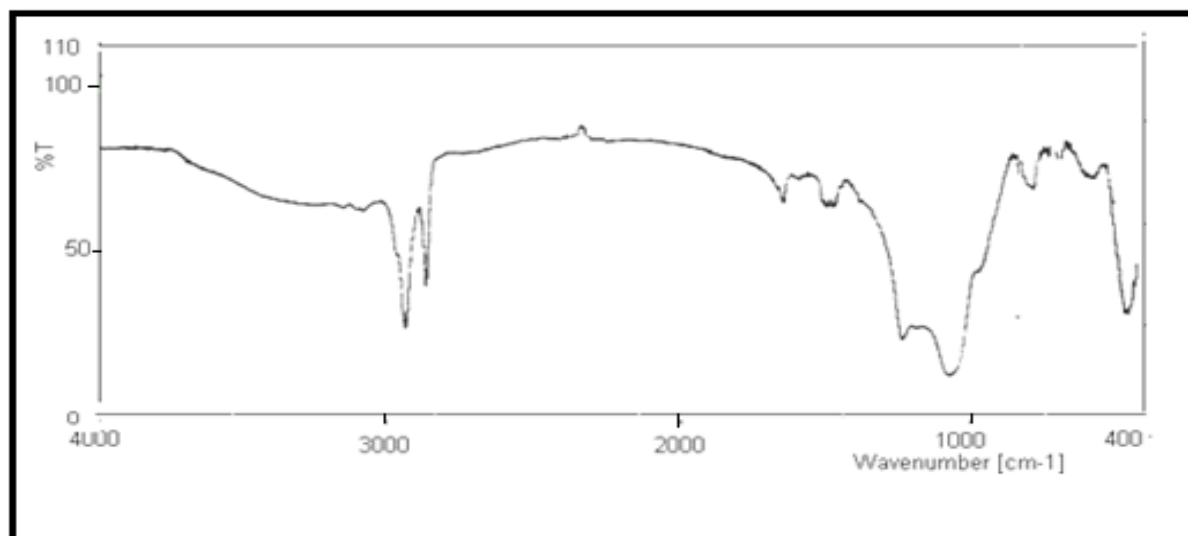


Fig. 4. IR spectrum C_{16} TMA-Kanemite.

Anti-bacterial activity of C_{16} TMA-kanemite against Staphylococcus aureus and Escherichia coli

The results in Table 2 show that C_{16} TMA-Kanemite has a good antibacterial effect against *Staphylococcus* by reducing after, 15 minutes, the optical density from 0.60 (control) to 0 (total destruction of bacteria).

After 5 minutes of contact of *Escherichia coli* with C_{16} TMA-kanemite we notice a considerable decrease in bacterial levels with an optical density of 0.530 to

0.213 Table 3. This rate remains almost constant because of the resistance of the bacteria Fig.7. The bactericidal effect of C_{16} TMA-kanemite on *Staphylococcus* as a result its alkyl group met quaternary ammonium since the increase of the alkyl chain of, quaternary ammonium is effective, on bacteria; positive cram, the efficiency of the quaternary Ammonium bacteria is directly related to their contact surface with, the environment of these microorganisms Fig. 6.

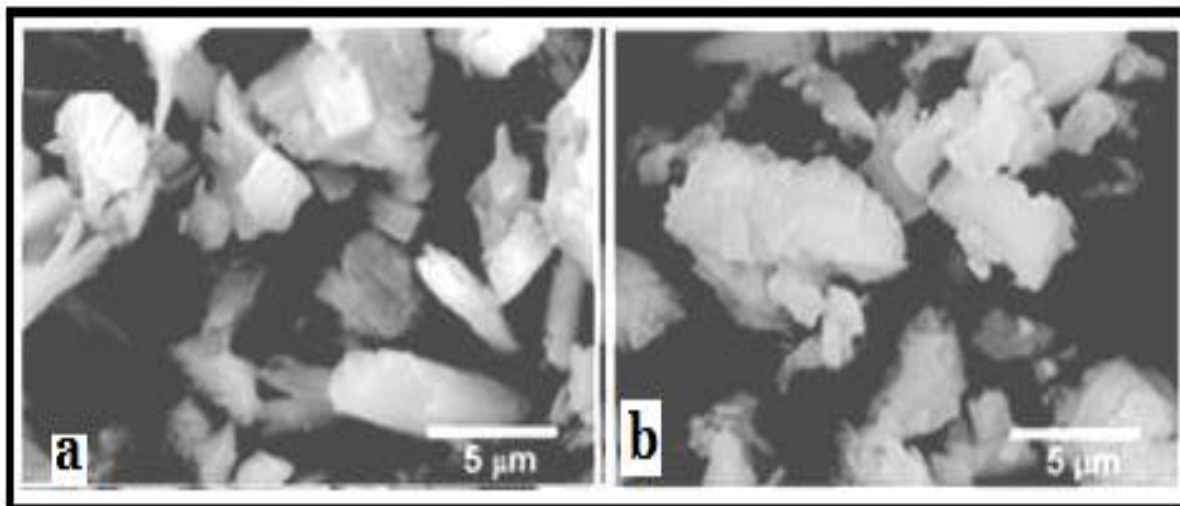


Fig. 5. SEM image (a) of kanemite, (b) C₁₆TMA-kanemite.

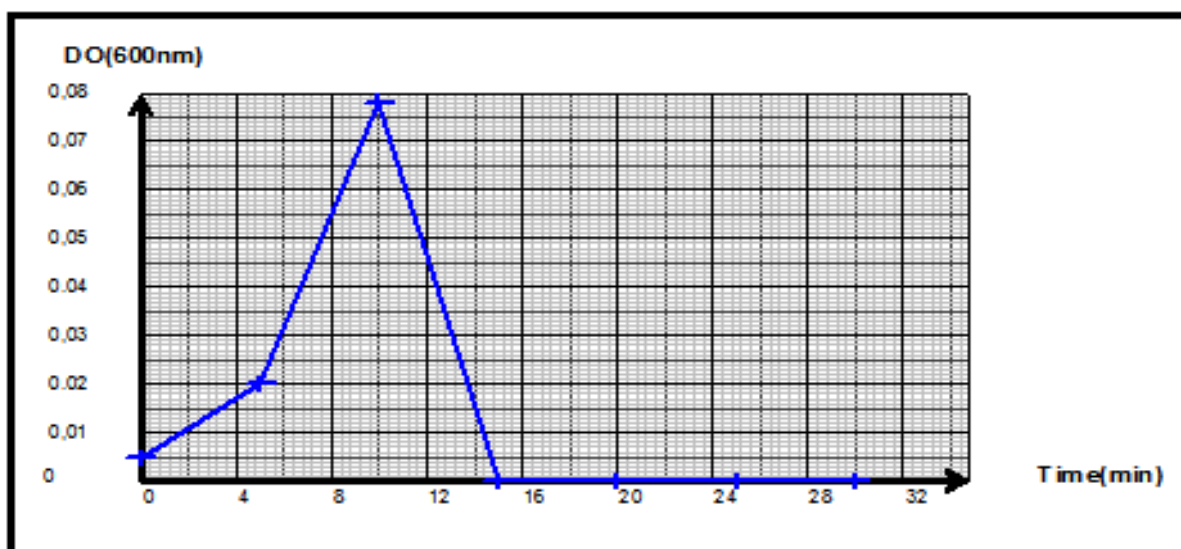


Fig. 6. Antibacterial activity of C₁₆ TMA-kanemite against *Staphylococcus aureus* as a function of time.

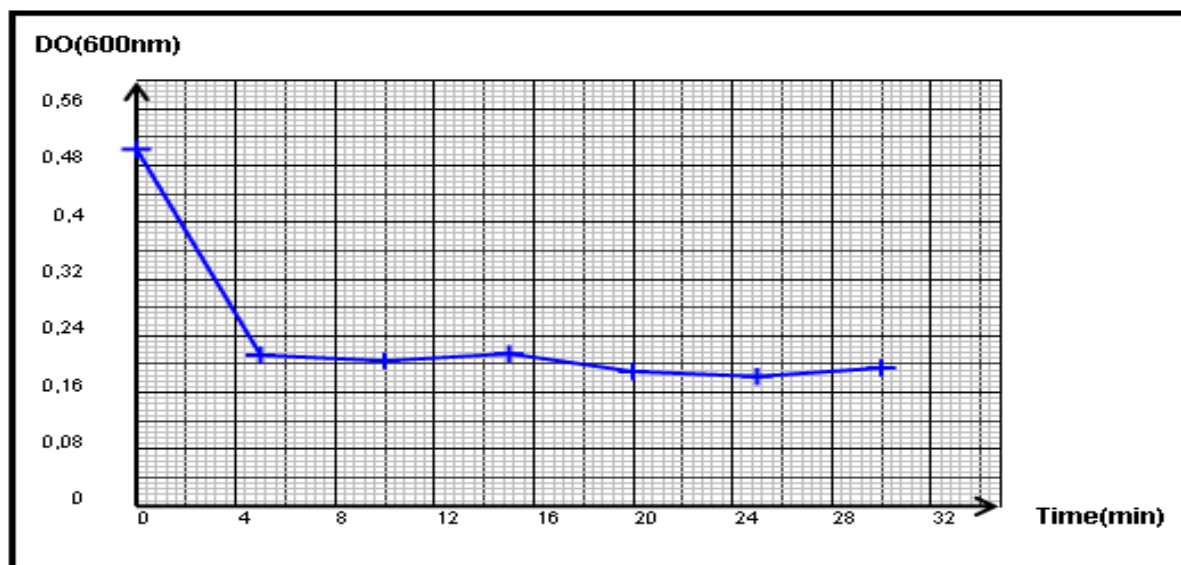


Fig. 7. Antibacterial activity of C₁₆ TMA-kanemite against *Escherichia coli* as a function of time.

Conclusion

This work leads us to compare the performances of the C16TMA-kanemite. In terms of eliminating bacteria that contribute to water contamination, such as *Staphylococcus aureus* and *Escherichia coli*. The results of the study of the antibacterial activity of C16TMA-kanemite against *Staphylococcus aureus* and *Escherichia coli* show an antibacterial effect of C 16 TMA-kanemite against *Staphylococcus* by a total destruction of the initial number of bacteria, the bactericidal effect of kanemite C16TMA is due to alkyl trimethylammonium. This amphiphilic structure and these surfactant properties, promotes the degradation of the cytoplasmic membrane of bacteria. C16TMA-kanemite can be adopted in water treatment to eliminate staphylococcal bacteria.

References

- Beneke K, Lagaly G.** 1977. Structural investigations of layered silicates by vibrational spectroscopy, *American Mineralogist* 762-763.
- Boukraa L, Benbarek H, Moussa A.** 2008. Synergistic action of starch honey against *Candida albicans* correlation with diastase number. *Brazilian Journal of Microbiology* 39(1), 40–43. <https://doi.org/10.1590/S1517838220080001000010>
- Gaudy C, Buxeraud J.** 2005. Antibiotiques; pharmacologie et thérapeutique .Publié par Elsevier Masson.
- Hamadi F, Latrache H, Mliji E, mallouki B.** 2009. Adhésion de *staphylococcus aureus* au verre et au teflon, *Revue de microbiology industrially, sanitaire, et environmental* 3(1), 1-16.
- Heinrich Thiesen P, Beneke K, Lagaly G.** 2002. Silylation of a crystalline silicic acid: an MAS NMR and porosity study. *Journal of Materials Chemistry* 12, 3010–3015. <https://doi.org/10.1039/B204314A>
- Herrera P, Burghardt RC, Phillips TD.** 2000. Adsorption of *Salmonella enteritidis* by cetyl peridinium exchanged montmorillonite clays. *Veterinary Microbiology* 74(3), 259-272 . [https://doi.org/10.1016/S0378-1135\(00\)00157-7](https://doi.org/10.1016/S0378-1135(00)00157-7)
- Jean P.** 1993. bacteries et environnement adaptation physiologique, presses universitaires de Grenoble.
- Johan Z, Maglione GF.** 1972. La kanemite, nouveau silicate de sodium hydrate ´ de ne oformation, *Bulletin de la Société française de Minéralogie et de Cristallographie* 95, 371–382.
- Kimura T, Itoh D, Okazaki N, Kaneda M, Sakamoto Y, Terasaki O, Sugahara Y, Kuroda K.** 2000. Lamellar hexadecyltrimethylammonium silicates derived from kanemite, *Langmuir* 16(20), 7624-7628. <https://doi.org/10.1021/la000325t>
- Ma YL, Xu ZR, Guo T, You P.** 2004. Adsorption of methylene blue on Cu(II)-exchanged montmorillonite, *Journal of Colloid and Interface Science* 280(2), 283–288. <https://doi.org/10.1016/j.jcis.2004.08.044>
- Ogawa M, Maeda N.** 1998. Intercalation of tris (2, 2 - bipyridine) ruthenium (II) into magadiite, *Clay Minerals* 33(4), 643–650.
- Ogawa M, Takizawa Y.** 1999. Intercalation of tris (2, 2 -bipyridine) ruthenium (II) into a layered silicate, magadiite, with the aid of a crown ether, *Journal of Physical Chemistry B*, 103(24), 5005–5009. <https://doi.org/10.1021/jp984198+>
- Okutomo S, Kuroda K, Ogawa M.** 1999. Preparation and characterization of silylated magadiites, *Applied Clay Science* 15(1-2), 253–264. [https://doi.org/10.1016/S0169-1317\(99\)00010-1](https://doi.org/10.1016/S0169-1317(99)00010-1)
- Ren Z, Zhang F, Yue L, Li X, Tao Y, Zhang G, Wu K, Wang C, Li B.** 2015. Nickel nanoparticles

highly dispersed in silica pillared clay as an efficient catalyst for chlorobenzene dichlorination, RSC Advances **5**, 52658-52666.

<https://doi.org/10.1039/C5RA05926G>

Rojo JM, Ruiz Hitzky E, Sanz J. 1988. Proton-sodium exchange in magadiite: spectroscopic study (NMR, IR) of the evolution of interlayer OH groups. Inorganic Chemistry **27(16)**, 2785-2790.

<https://doi.org/10.1021/ic00289a009>

Ruiz Hitzky E, Aranda P, Darder M, Ogawa M. 2011. Hybrid and biohybrid silicate based materials: molecular vs. block-assembling bottom-up processes. Chemical Society Reviews **40**, 801-828.

<https://doi.org/10.1039/C0CS00052C>

Wang Q, Zhang Y, Zheng J, Wang Y, Hu T, Meng C. 2017. Metal oxide decorated layered silicate magadiite for enhanced properties: insight from ZnO and CuO decoration, Dalton Trans **46**, 4303-4316.

<https://doi.org/10.1039/C7DT00228A>

Wang Q, Zhang Y, Zheng J, Hu T, Meng C. 2017. Synthesis, structure, optical and magnetic properties of interlamellar decoration of magadiite using vanadium oxide species. Microporous and Mesoporous Materials **244**, 264-277.

<https://doi.org/10.1016/j.micromeso.2016.10.046>

Yamada Z, Ohta K, Takeuchi S, Suzuki K, Mori T. 1991. Preparation and properties of antibacterial clay interlayer compound. Kagaku Kagaku Ronbunshu **17**, 29-34.